A PROJECTIVE THERMOSTATTING DYNAMICS TECHNIQUE

ZHIDONG JIA* AND BENEDICT J. LEIMKUHLER †

Abstract. A dynamical framework is developed with several variations for modeling multiple timescale molecular dynamics at constant temperature. The described approach can be adapted to various applications, including mixtures of heavy and light particles and models with stiff potentials. Canonical sampling properties are proved under the ergodicity assumption. Implications for numerical method development are discussed and the technique is validated in numerical experiments with model problems, including a simple model of a diatomic gas with anharmonic weak interaction.

Key words. thermostat, constant temperature molecular dynamics, Nosé-Hoover, Nosé-Poincaré, multiple timescale simulation, nonequilibrium dynamics, canonical sampling, symplectic integrator, Hamiltonian systems, time-reversible, slow dynamics, adiabatic separation, reversible averaging

AMS subject classifications. 65P10, 70-08, 70K70, 74A15, 82-08, 82B30, 82C05

1. Introduction.

Multiple timescale problems arise in many research fields such as climatology and molecular dynamics [35, 31, 7, 12, 23]. Although the micro-scale quantities are generally of no particular interest, they impose a severe restriction on the time stepsize for the numerical simulation of the whole system. As a result the calculation of macro-scale quantities, which accounts for most of the simulation time, will induce large computational overhead at very small time stepsize for a long-term numerical integration. Theoretical model simplification or reduction has been suggested to improve the situation. Depending on the type of system, deterministic or stochastic reduced models can be obtained by eliminating or replacing the fast components. Examples include the averaging method in celestial mechanics [1], the time homogenization technique for classical mechanics with stiff potentials [31, 7], and the molecular theory of Brownian motion [28, 36, 11]. These formalisms can be combined with specialized numerical methods. An alternative—purely numerical—approach is to seek a multiple timescale method which introduces an on-the-fly averaging procedure to compute the effective slow dynamics [15, 13, 24]. For the systems where it is applicable, this type of method has potential for adaptive resolution of solution features and more accurate long-term simulation.

The selection of modeling formulation for molecular dynamics at constant temperature is application dependent. Generally speaking, there are two fundamental perspectives depending on whether the emphasis is placed on sampling or on the recovery of dynamical information associated to certain degrees of freedom, typically in the presence of rapidly equilibrated subdynamics. As an illustration, consider the problem of relaxation in systems with fast vibrational components. Many physical problems, such as polyatomic gases and biomolecules, consist of both slow translational and fast vibrational degrees of freedom. A major historic challenge to understanding of such systems arises from the fact that the equipartition principle of statistical mechanics doesn't agree with ordinary experiments. At the turn of the 19th century, Boltzmann [5] and Jeans [16, 17] proposed a possible solution and conjectured that the time scale for fast vibrational modes to share their energy might grow exponentially with the vibrational frequency, i.e. high frequencies are essentially

*Institute of Computational Mathematics, Chinese Academy of Sciences (CAS), Beijing 100080, CHINA (zj4@mcs.le.ac.uk).

†Centre for Mathematical Modelling, Mathematics Building, University of Leicester, LE1 7RH, UK (b.leimkuhler@mcs.le.ac.uk).

decoupled, and thus frozen. Benettin *et al.* [4] observed, in numerical experiments for a simplified diatomic gas model, that equilibrium is rapidly obtained for the translational degrees of freedom, while a much longer time, increasing exponentially with frequency, is required to observe an appreciable energy sharing for the fast vibrational degrees of freedom. On realistic timescales, the detailed evolution of adiabatic vibrational components can be viewed as having no direct impact on the slow dynamics, and energy exchanges with fast vibrational degrees of freedom are too small to contribute to thermal equilibration of the whole system. Based on this perspective, it is natural to employ an artificial thermostatting technique so as to accelerate the energy exchange for the vibrational components and attain the thermal equilibration for the whole system. In this way we gain the potential to recover thermodynamic properties of interest on a computer-accessible time scale. On the other hand, many models in molecular simulation incorporate a nonlinear and ergodic bath that easily relaxes to thermal equilibrium. The challenge may then be to obtain canonical sampling of a system in which the slow variables, not the fast ones, are not rapidly equilibrated on the timescale of interest. In these models, a thermostat can be used to improve ergodicity of the slow variables and thus enhance sampling, but extended variable thermostatting may not be necessary or desirable in the fast variables.

Given the two potential purposes of molecular simulation outlined in the above examples, a fundamental mathematical question arises: can we find a sensible method to thermostat a system in favor of one or the other modeling perspective? Our solution is to thermostat the system using a projection technique designed to separate the degrees of freedom. Since the temperature is associated with the kinetic energy, we may adjust the momenta projection in some suitable way in order to coincide with the modeling perspective, thermostatting either the slow or fast components. This procedure is not entirely straightforward. If we wish to avoid introducing additional, nonphysical coupling of fast and slow degrees of freedom (which would complicate the construction of numerical methods), we must employ an appropriate time reparametrization scheme. If the ergodicity of the thermostatted system cannot be assumed, chains may be needed in order to obtain proper sampling. Our preference is to work always with a Hamiltonian model, allowing the use of symplectic integrators with provable theoretical and practical benefits, but this is not always possible. In certain cases, a mixed technique, in which a critical part of the system is treated as an adiabatically perturbed Hamiltonian system, may be of use. We outline such techniques.

In the next section, we derive a general projective thermostatting dynamics (**PTD**), showing that it recovers canonical sampling under the assumption of ergodicity. This formulation is not suited for direct numerical simulation, due to the artificial time-scaling which can cause numerical difficulty. Resolving that difficulty calls for incorporation of an appropriate time-transformation, and this must be done differently in different modeling contexts. In Section 3, we study a special example of **PTD**, which describes the thermostatting of the adiabatic fast degrees of freedom (**DOF**), and the relevant dynamical and sampling characteristics have been analyzed. Finally Section 4 contains some comments on numerical methods and numerical experiments. Detailed treatment of discretization issues is left for a future article.

2. A Projective Formulation for Partial Thermostatting. In the sequel, we consider multiple timescale systems described by a Hamiltonian function of the

following form:

$$H = \frac{p^T M^{-1} p}{2} + V(q) + \sigma U(q), \tag{2.1}$$

where M is a mass matrix and σ is a constant. For the sake of clarity and illustration, we refer to two model settings, corresponding to the examples below:

Example 1: Strong and Weak Potentials. In this case we have $\sigma = \frac{1}{\epsilon^2}, \epsilon \ll 1$, and σU may be used to represent the strong potential term associated with restraints such as bond length and bond angle in molecular dynamics. The mass matrix is simply assumed to be bounded. We assume that U can be decomposed as a sum of squares as

$$U(q) = \sum_{i=1}^{R} \left[\mathcal{U}^i(q)\right]^2. \tag{2.2}$$

For later reference, we introduce a critical manifold [7]

$$\mathcal{N} = \{q \in \mathcal{M} | \mathcal{U}(q) = 0\}, \tag{2.3}$$

where $\mathcal{U} = \left[\begin{array}{cccc} \mathcal{U}^1 & \mathcal{U}^2 & \dots & \mathcal{U}^R \end{array} \right]^T$ and $\mathcal{M}$ is the whole configuration space. The tangent space $T_q\mathcal{N}$ can be defined as

$$T_q\mathcal{N} = \{p | \mathcal{U}'(q)p = 0\}. \tag{2.4}$$

Example 2: Slow and Fast Variables. Consider a mixture of heavy and light particles with a corresponding natural separation of the degrees of freedom. To retain constant temperature, the whole system is immersed in a heat bath. In this case, we take $\sigma = 0$ and the mass matrix as well as momenta, related with fast and slow variables, can be decomposed as

$$M = \left(\begin{array}{cc} M_f & 0 \\ 0 & M_s \end{array} \right), \quad p = (p_f^T, p_s^T)^T. \tag{2.5}$$

We suppose $\| M_f \| \ll \| M_s \|$. The Hamiltonian function can be rewritten as

$$H = \frac{p_f^T M_f^{-1} p_f}{2} + \frac{p_s^T M_s^{-1} p_s}{2} + V(q). \tag{2.6}$$

Other categories of problems admitting a slow-fast variable decomposition arise through application of the quasi-continuum formulation [34] and similar models for materials.

2.1. Momenta Decomposition. Let a projector $\mathcal{P}$ be given and consider the momenta decomposition

$$p = \mathcal{P}p + \mathcal{Q}p, \tag{2.7}$$

where $\mathcal{Q} = I - \mathcal{P}$. The original Hamiltonian function can be rewritten as

$$H = \frac{p^T \mathcal{P}^T M^{-1} \mathcal{P} p}{2} + \frac{p^T \mathcal{Q}^T M^{-1} \mathcal{Q} p}{2} + V(q) + \sigma U(q), \tag{2.8}$$

where we have made the "*orthogonality assumption*":

$$\mathcal{P}^T M^{-1} \mathcal{Q} = 0. \tag{2.9}$$

Such a projection arises naturally in each of the two example contexts mentioned above. In the case of the system with identified strong and weak potentials as in Example 1, we define $\mathcal{P}$ by

$$\mathcal{P} = M^{1/2}\mathcal{A}M^{-1/2} = G^T(GM^{-1}G^T)^{-1}G, \tag{2.10}$$

where $G = \mathcal{U}'(q)$. Observe that this is orthogonal to its complement $I - \mathcal{P}$ with respect to the $M^{-1/2}$-weighted inner product, as required.

For the model of Example 2, the situation is even simpler. We introduce

$$\mathcal{P} = \begin{pmatrix} 0 & 0 \\ 0 & I \end{pmatrix}, \tag{2.11}$$

which can be obtained from (2.10) by assuming $G = \begin{bmatrix} 0 & I \end{bmatrix}$.

In each case the projection is easily seen to identify the fast (or slow) part of the conjugate momenta, which can be viewed as a specific subset of the generalized coordinates.

2.2. Projective Thermostatting. Next, we observe that the Nosé thermostatting technique can be applied to the $\mathcal{P}$-projected momenta only, resulting in a "projective thermostatting" formulation described by the following Hamiltonian function:

$$\mathcal{H}_{Nosé} = \frac{p^T\mathcal{P}^TM^{-1}\mathcal{P}p}{2s^2} + \frac{p^T\mathcal{Q}^TM^{-1}\mathcal{Q}p}{2} + V(q) + \sigma U(q) + \frac{\pi^2}{2\mu} + g_f k_B T \ln s. \tag{2.12}$$

Here g_f is determined as the rank (or trace) of the projector $\mathcal{P}$. We prove the following theorem regarding this extended Nosé-like Hamiltonian:

THEOREM 2.1. *The microcanonical density function corresponding to (2.12), when integrated with respect to the auxiliary thermostatting variables, reduces to the canonical density distribution $e^{-\frac{1}{k_BT}H}$ in the physical variables.*

Proof. We would like to carry out a reduction of distribution from the extended phase space (of variables p, q, s, π) into (p, q)-space such that the canonical density distribution is obtained. The partition function can be written as

$$Z = \int dpdqdsd\pi\delta(\mathcal{H}_{Nosé} - \mathcal{H}_0). \tag{2.13}$$

First, we take the momenta transformation $p \to M^{-1/2}p = \bar{p}$, then define

$$\mathcal{A} = M^{1/2}\mathcal{P}^TM^{-1}\mathcal{P}M^{1/2}, \tag{2.14}$$

which is a symmetric projection matrix. The additional constant C_0 induced by the momenta transformation can be put into the partition function. The transformed Hamiltonian can be written as

$$\bar{\mathcal{H}}_{Nosé} = \frac{\bar{p}^T\mathcal{A}\bar{p}}{2s^2} + \frac{\bar{p}^T\mathcal{B}\bar{p}}{2} + V(q) + \sigma U(q) + \frac{\pi^2}{2\mu} + g_f k_B T \ln s, \tag{2.15}$$

where $\mathcal{B} = I - \mathcal{A}$. Since $\mathcal{A}$ is idempotent and symmetric, the Schur matrix decomposition theorem assures

$$W^T\mathcal{A}W = \begin{pmatrix} I & 0 \\ 0 & 0 \end{pmatrix}. \tag{2.16}$$

We thus take the momenta transformation $\bar{p} \to W\bar{p} = \tilde{p}$, which doesn't affect the value of integral since the Jacobian matrix W of this transformation is orthogonal, with unit determinant. The partition function can be rewritten as

(2.17)
$$Z = C_0 \int d\tilde{p}_1 d\tilde{p}_2 dq ds d\pi \delta \left(\frac{\tilde{p}_1^T \tilde{p}_1}{2s^2} + \frac{\tilde{p}_2^T \tilde{p}_2}{2} + V(q) + \frac{1}{\epsilon^2} U(q) + \frac{\pi^2}{2\mu} + g_f k_B T \ln s - \mathcal{H}_0 \right).$$

Integrating out the thermal variables s, π by the usual procedure [29], and letting C_1 be the associated constant, we obtain:

$$Z = C_0 C_1 \int d\tilde{p} dq e^{-\frac{1}{k_B T}\left(\frac{\tilde{p}^T \tilde{p}}{2} + V(q) + \sigma U(q)\right)}, \tag{2.18}$$

which, by the back-transformation $\tilde{p} \to M^{1/2} W^T \tilde{p} = p$, is formulated as

$$Z = C_1 \int dp dq e^{-\frac{1}{k_B T}\left(\frac{p^T M^{-1} p}{2} + V(q) + \sigma U(q)\right)} = C_1 \int dp dq e^{-\frac{1}{k_B T} H}. \tag{2.19}$$

Thus, the canonical density distribution

$$\rho = e^{-\frac{1}{k_B T} H} \tag{2.20}$$

is obtained. □

Although the above-mentioned Hamiltonian formulation appears to be sensible from a theoretical perspective, it introduces numerical instability in practical applications due to the potential for sampling small values of the thermostatting variable s (which will be sampled thoroughly if the system is ergodic). A standard way to resolve this numerical difficulty is to employ a time reparametrization. However, the use of a time transformation in the multiple timescale model can introduce additional coupling between the scales, which will at best complicate the development of a multiscale numerical method. A key point is therefore to model the system without destroying the multiple timescale structure which facilitates the construction of efficient numerical methods. The modeling perspective will determine the way in which we scale the time variable, as we detail in the next two subsections.

2.3. Projective Thermostatting of Slow Components. If we introduce the thermostat in the slow variables, the thermostatting variables should be of slow time scale. Without altering the separation of time scale, we can introduce a Hamiltonian formulation (**PTD-I**)

(2.21)
$$\mathcal{H}_{NP} = s \left(\frac{p^T \mathcal{P}^T M^{-1} \mathcal{P} p}{2} + \frac{p^T \mathcal{Q}^T M^{-1} \mathcal{Q} p}{2s^2} + V(q) + \sigma U(q) + \frac{\pi^2}{2\mu} + g k_B T \ln s - \mathcal{H}_0 \right).$$

The introduction of time-rescaling in this way does not alter the sampling of the canonical ensemble, as is easily assured by consideration of the proof of Theorem 2.1.

COROLLARY 2.2. *Provided ergodicity is assumed, the system corresponding to (2.21) recovers the canonical ensemble.*

For this case a numerical method can be constructed according to the Hamiltonian splitting:

$$\mathcal{H}_1 = s \left(\frac{p^T \mathcal{P}^T M^{-1} \mathcal{P} p}{2} + \sigma U(q) - \mathcal{H}_0 \right), \tag{2.22}$$

$$\mathcal{H}_2 = s \left(\frac{p^T \mathcal{Q}^T M^{-1} \mathcal{Q} p}{2s^2} + V(q) + \frac{\pi^2}{2\mu} + g k_B T \ln s \right). \tag{2.23}$$

$\mathcal{H}_1$ can be integrated with small stepsize while $\mathcal{H}_2$ would require a larger one. The same principle would apply in considering more sophisticated multiscale schemes such as those described in [15, 24].

2.4. Projective Thermostatting of Vibrational Modes. The above technique will not work if our interest is in thermostatting of the fast variables of a multiscale model, since we must then take the thermostatting variable to be fast and scale separation will be destroyed. Here we show that it is possible to use Nosé-Hoover dynamics to thermostat just a particular subset of the components of the system, while maintaining a single timescale. A key point is that we are able to apply the scheme in the original system variables.

Through a symplectic transformation $p \to M^{-1/2}p, q \to M^{1/2}q$, the Hamiltonian (2.1) can be rewritten in the form:

$$H(p,q) = \frac{p^T p}{2} + V(q) + \sigma U(q). \tag{2.24}$$

This transformation simplifies further analysis. Our idea is that we identify the slow and fast variables by employing a canonical phase transformation, and then the identified fast variables corresponding to the original vibrational modes can be thermostatted by use of e.g. Nosé-Hoover dynamics. The reader may refer to the **Appendix A** for the details. The re-formulation into original coordinate finally results in the following dynamics (**PTD-II**):

$$\dot{q} = M^{-1}p, \tag{2.25}$$

$$\dot{p} = -\nabla_q V(q) - \sigma \nabla_q U(q) - \frac{\xi}{\mu}\mathcal{P}p, \tag{2.26}$$

$$\dot{\xi} = p^T M^{-1}\mathcal{P}p - \mathrm{trace}(\mathcal{P})k_B T, \tag{2.27}$$

where the projection operator $\mathcal{P}$ is

$$\mathcal{P} = M^{1/2}\mathcal{A}M^{-1/2} = G^T(GM^{-1}G^T)^{-1}GM^{-1}. \tag{2.28}$$

In the extreme case of separated fast and slow components, the projection operator in the above formula can be written as

$$\mathcal{P} = \begin{pmatrix} 0 & 0 \\ 0 & I \end{pmatrix}, \tag{2.29}$$

This formulation, although not Hamiltonian, has some desirable features in the setting of applications.

THEOREM 2.3 (Galilean Invariance [1]). *Given that the potentials $V(q), U(q)$ are invariant with respect to Galilean transformations, the dynamics (2.25)-(2.27) have the following geometric invariants:*

1. **Separation of strong and weak potential** *Galilean time and space invariance: time reversibility, conservation of total linear momenta, Conservation of angular momenta, conservation of pseudo-energy, vector fields in terms of relative positions and velocities only.*
2. **Separation of fast and slow variables** *Galilean time invariance: time reversibility, conservation of pseudo-energy.*

[1] The dynamics must be invariant with respect to Galilean transformations such as time, uniform motion, translation and rotation.

Here the pseudo-energy

$$H_T(p,q,\xi) = \frac{p^T M^{-1} p}{2} + V(q) + \sigma U(q) + \frac{\xi^2}{2\mu} \tag{2.30}$$

is obtained by combining the dynamics (2.25)-(2.27) together with an independent equation

$$\dot{\eta} = \frac{\xi}{\mu}. \tag{2.31}$$

Finally, we prove:

THEOREM 2.4. *Provided ergodicity is assumed, the dynamics of (2.25)-(2.27) recover the canonical ensemble distribution*

$$f(q,p,\xi) = Ce^{-\frac{1}{k_B T} H_T}, \tag{2.32}$$

where C is a constant.

Proof. The Liouville equation for the dynamics can be written as

$$\frac{df}{dt} = -(\frac{\partial}{\partial \Gamma} \cdot \dot{\Gamma}) f = \frac{\xi}{\mu} \cdot \mathrm{trace}(\mathcal{P}) f, \tag{2.33}$$

where

$$\Gamma = (q,p,\xi). \tag{2.34}$$

On the other hand, we utilize

$$\frac{d}{dt} H_T = -\frac{\xi}{\mu} g_f k_B T, \tag{2.35}$$

then

$$\frac{df}{dt} = -\frac{1}{k_B T} \frac{dH_T}{dt} f, \tag{2.36}$$

whose solution is exactly the desired canonical ensemble distribution. It should also be noticed that $\mathrm{trace}(\mathcal{P})$ is independent of q and equal to the codimension of the critical manifold, which is exactly the number of independent constraints. □

REMARK 1. *Moreover, if we would like to thermostat both slow and fast components simultaneously but separately, a dynamics with two thermostats can be formulated as*

$$\dot{q} = M^{-1} p, \tag{2.37}$$

$$\dot{p} = -\nabla_q V(q) - \sigma \nabla_q U(q) - \frac{\xi}{\mu} \mathcal{P} p - \frac{\zeta}{\nu} \mathcal{Q} p, \tag{2.38}$$

$$\dot{\xi} = p^T M^{-1} \mathcal{P} p - \mathrm{trace}(\mathcal{P}) k_B T, \tag{2.39}$$

$$\dot{\zeta} = p^T M^{-1} \mathcal{Q} p - \mathrm{trace}(\mathcal{Q}) k_B T, \tag{2.40}$$

which is of the same sampling and conservative properties mentioned above.

3. A Special Case: Beyond Equilibrium. The idea of thermostatting part of a system can be used for sampling, as we have seen above, but it may have deeper ramifications. In this section, we restrict attention to the model of Example 2, and suppose that light and heavy particles achieve thermal equilibrium in different ways: the heat bath is assumed to actively contact the light particles, while the slow particles exchange energy by interacting with the light particles. We will construct a mathematical formulation which comprises a direct thermostatting device for the light particles and a conservative coupling between the light and heavy particles. The time transformation is employed only in the subdynamics of fast variables, as follows (**PTD-III**):

$$\dot{Q} = M^{-1}P, \tag{3.1}$$

$$\dot{P} = -\nabla_Q V(q,Q), \tag{3.2}$$

$$\dot{q} = \frac{m^{-1}p}{s}, \tag{3.3}$$

$$\dot{p} = -s\nabla_q V(q,Q), \tag{3.4}$$

$$\dot{s} = s\frac{\pi}{\mu}, \tag{3.5}$$

$$\dot{\pi} = \frac{p^T m^{-1} p}{s^2} - g_f k_B T - \triangle\mathcal{H}, \tag{3.6}$$

where

$$\triangle\mathcal{H} = \frac{P^T M^{-1} P}{2} + \mathcal{H}^{[f]}_{Nosé} - \mathcal{H}_0, \tag{3.7}$$

$$\mathcal{H}^{[f]}_{Nosé} = \frac{p^T m^{-1} p}{2s^2} + V(q,Q) + \frac{\pi^2}{2\mu} + g_f k_B T \ln s, \tag{3.8}$$

and g_f is equal to the number of degrees of freedom of the light particles, $\mathcal{H}_0$ is given by $\frac{P^T M^{-1} P}{2} + \mathcal{H}^{[f]}_{Nosé}$ at initial values.

The following results are immediate:

THEOREM 3.1 (Incompressibility and first integral). *The dynamics (3.1)-(3.6) are divergence-free, and have the following first integral*

$$s\triangle\mathcal{H} = s\left(\frac{P^T M^{-1} P}{2} + H^{[f]}_{Nosé} - \mathcal{H}_0\right). \tag{3.9}$$

COROLLARY 3.2. *Assuming ergodicity of (3.1)-(3.6) on the surface of constant integral (3.9), sampling with respect to the canonical ensemble can be recovered from the trajectories of (3.1)-(3.6). (A similar proof can be referred to [6].)*

A crucial aspect is that the slow subdynamics present long term non-equilibrium behavior, however the fast subdynamics are assumed to converge to the thermal equilibrium rapidly along the adiabatic change of slow variables. If there is a weak coupling between the heavy and light particles, we could expect very long time non-equilibrium behavior for the heavy particles. Then we are not interested so much in determining the statistical properties of the slow variables, but in capturing a realistic dynamical evolution. By introducing a potentially more realistic heat bath interface model in the slow variables, the dynamics suggests a way to shield the system of interest from the artificial characteristics of Nosé-like dynamics, since the dynamics preserve, in some sense, the natural Newtonian interaction between the heavy and light particles.

Due to the partial use of Poincaré time transformation, the whole system is *not* Hamiltonian any more, and our point of view is rather that the fast subdynamics are Hamiltonian in terms of slow-varying Q, P, which hopefully enables a more stable symplectic numerical integration for the thermalized fast subdynamics.

It should be noted that the dynamics subject to (3.1)-(3.6) and (3.7) are quite different from the usual constant temperature dynamics. We traditionally consider the thermostatting as being introduced by one degree of freedom, a so-called "global demon" [22]. This thermal DOF interacts directly with every degree of freedom in the original system. The dynamics we suggest only applies the thermostatting to the fast dynamics while achieving the desired canonical density function for the whole system. Moreover, the realistic dynamics agree with our setup of the molecular model, and coincide very well with our physical viewpoint on the interaction among the heat bath, light and heavy particles.

In [29], Nosé explained a sort of multi-thermostatting Nosé-Hoover dynamics which suggests a formulation in some ways similar to ours, and such multiple thermostatting or partial thermostatting methods have been implemented on an ad-hoc basis (see e.g. [26] for a method which incorporates a thermostatting of bond vibrations only) and found to be effective. However, there are significant differences between the Nosé-like approach and that presented here: for the fast dynamics, the proposed formulation retains the correct structure of an adiabatically perturbed Hamiltonian system. In addition, our method introduces a direct dependency in the differential equations for the fast variables on the slow momenta, as well as on positions.

We also wish to comment on the fluctuation of total linear momenta in our model. As is well known, a conservative molecular dynamics will preserve total linear momenta due to Newton's third law. One natural question is: should a system with temperature control conserve linear momenta? From a modeling perspective, we envision our system immersed in a larger system, subject to a complete dynamics described by a Hamiltonian

$$H(Q,q,q_h,P,p,P_h) = \frac{P^T M^{-1} P}{2} + \frac{p^T m^{-1} p}{2} + \frac{p_h^T m_h^{-1} p_h}{2} + V(q,Q) + U(q,q_h),$$

where q_h, p_h are conjugate heat bath variables, m_h is the mass matrix of the heat bath particles and $U(q,q_h)$ represents the interaction of heat bath particles and the light particles. In this context, the dynamics of Q,q,P,p is obviously not closed, and the heat bath will exert (effectively) an external force on the open dynamics. In our model, we replace the heat bath interaction by a simplified dynamics, but the purpose is ultimately the same.

We therefore neither expect nor desire conservation of total linear momenta for the dynamics interacting with heat bath. Instead, we can easily show (based on the results in Section 2) that, under assumption of ergodicity, the *average* of total linear momenta is equal to zero. This implies that Newton's third law is valid from a macroscopic point of view in our circumstance. The situation here is similar to that of Langevin dynamics, where, also, the total momenta fluctuates microscopically but with the correct average value. The magnitude of fluctuation will be dependent on how strong the heat bath interacts with the dynamics concerned. Although we model the fast subdynamics by artificial Nosé dynamics, we still retain the correct dynamics of slow particles in the sense that there is a realistic interaction between the fast and slow subdynamics and sampling is only assumed with respect to the fast subdynamics.

Our approach should be distinguished from the setting of pure Nosé dynamics, which is justified in terms of sampling properties rather than as a possible dynamical description of the slow system. (In this sense, the article [9], which addresses conservation of the total "virtual" momenta, is unrelated.)

4. Numerical Issues. In summary, we have derived various kinds of thermostatting molecular dynamics, which are constructed by introducing the thermostat for the projective modes consistent with our modeling perspectives. In the following, we will discuss two simplified models to validate our theoretical analysis.

4.1. Algorithms. We would like to use a specially designed numerical integrator to efficiently resolve the evolution of the models described in this article by taking advantage of the scale separation. A candidate method is the reversible averaging method of [24], but since the fast subsystem in **PTD-III** involves not only the slow variable Q but P, the direct application of this method is not possible, so a generalization of this method is needed, comprising the three essential procedures:

Averaging Compute the fast subdynamics in time with fixed slow variables for a fixed time interval to obtain a trajectory $q(t)$, along which the averaged force $\langle -\nabla_Q V(q(t), Q)\rangle$ can be calculated.

Slow Propagation The slow subdynamics is evolved with the averaged force due to fast variables.

Fast Propagation Simulation of the fast subdynamics with an interpolation of slow variables.

In terms of computational efficiency compared to standard schemes like Verlet or variants thereof, this approach is of particular interest when the cost of slow forces (force components due to interactions among the slow variables only) is dominant. In these cases, the method promises to reduce the frequency of slow force evaluations, while stably resolving the fast dynamics. The resonance-breaking property of the reversible averaging method compared to schemes like multiple timestepping was established in [24] and is based on the combination of averaging (i.e. smoothing) the effect of the fast variables on the slow, while introducing a time-dependent slow evolution in the fast propagation.

Some details regarding the implementation of the Generalized Reversible Averaging numerical method are provided in **Appendix B**.

4.2. Biharmonic model. Our first model system is described by the Hamiltonian

$$H = \frac{P^2}{2M} + \frac{p^2}{2m} + \frac{kq^2 + (q-Q)^2}{2} \tag{4.1}$$

with temperature control provided by partial thermostatting methods based on the Nosé-Poincaré chain of **Appendix C**. A chain formulation of this type is needed to obtain ergodic sampling in low-dimensional models such as this.

In the first instance we used the same frequency for both variables. The good convergence of the distribution of the momenta is illustrated in Figures 4.1 and 4.2. Here we have taken $Rm_2 = 0.08; Rm_3 = 0.04; Rm_4 = 0.02; Rm_5 = 0.01; Tm_1 = 0.5; Tm_2 = 1.0; Tm_3 = 1.0; Tm_4 = 1.0; Tm_5 = 1.0; \delta t = 0.01; M = m = 1.0; k = 1.0$. Obviously, the momenta p has faster convergence of distribution than P. The results show that we succeed in getting thermal equilibrium for the full system by partial thermostatting. In this case, the ergodicity assumption appears to be valid.

We next considered the biharmonic model with frequencies 1,10. We found that the stability threshold for a generalized leap-frog method, which comprises the Verlet

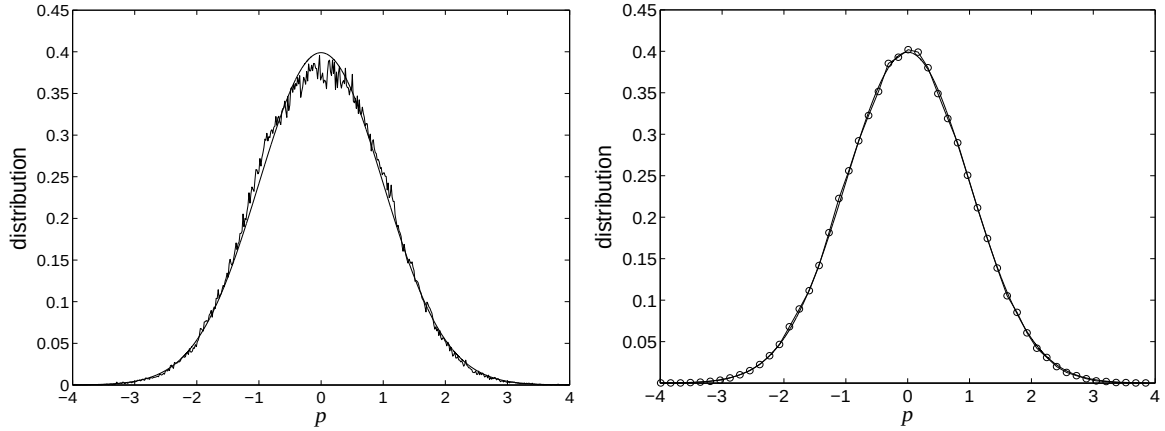

FIG. 4.1. *The convergence of distribution for the momentum p in the strong coupling case, running 400,000 (left) and 4M (right) time steps with* $\delta t = 0.01$.

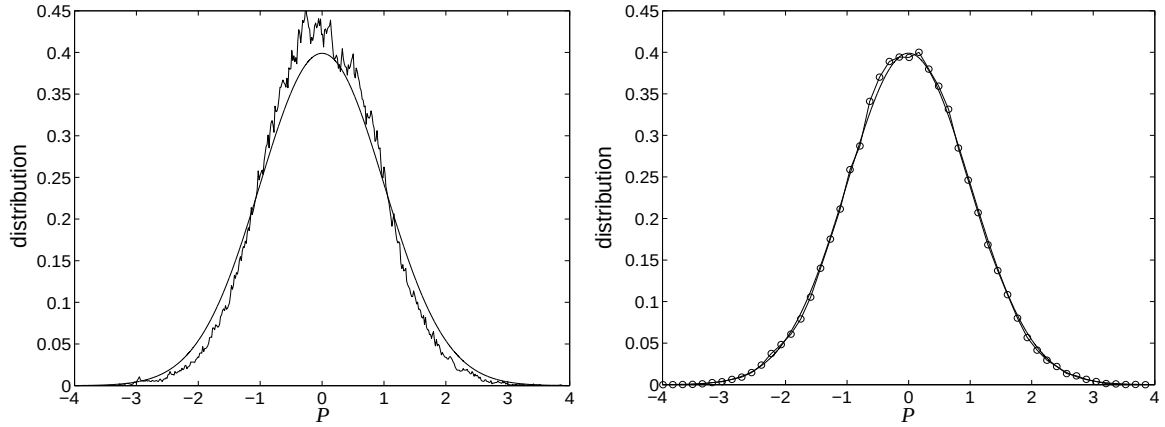

FIG. 4.2. *The distribution for the momentum P in the strong coupling case, running 400,000 (left) and 4M (right) time steps with* $\delta t = 0.01$.

method for slow subdynamics and a Hamiltonian splitting method for fast subdynamics, is near $\delta t = 0.005$.

We have used a generalized reversible averaging method. Excellent conservation of the first integral was obtained with stepsize $\delta t = 0.03$, as shown in Figure 4.3. Compared with the stepsize threshold $\delta t = 0.005$ of the generalized leap-frog method, the stepsize $\delta t = 0.03$ represents a substantial improvement in the handling of the slow dynamics.

We observed similar good conservation of the first integral in many experiments with stepsizes smaller than $\delta t = 0.03$ and no evidence of stepsize resonance. Results of some 500 simulations with long stepsizes in the range $[0.002, 0.03]$ (using stepsizes for fast dynamics fixed well below the fast stability threshold) are summarized in Figure 4.6.

In Figure 4.4, we see the very rapid convergence of distribution of the fast momentum p. However, the distribution of slow momentum P in Figure 4.5 shows no

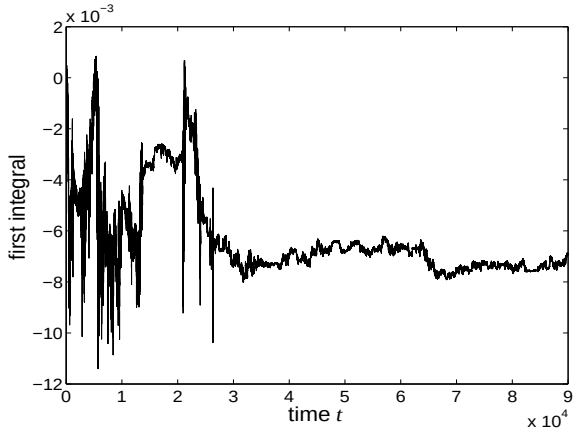

FIG. 4.3. *The error of first integral* $s\triangle\mathcal{H}$ *for* ***GRA*** *method,* $\delta t = 0.03$.

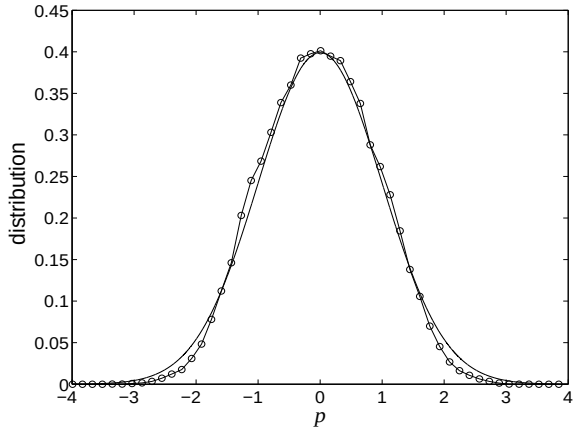

FIG. 4.4. *The distribution of fast momentum p for* ***GRA*** *method in the weak coupling case, 1M time steps with* $\delta t = 0.03$.

evidence of convergence. We examined the phase space trajectories of the slow subdynamics for both the same-frequency and different-frequency cases observing that the slow momentum in different-frequency case is bounded in the interval $[-2.5, 2.5]$ approximately. The fast and slow dynamics in this problem differ in frequency by an order of magnitude in this example. In this setting, we do not expect the thermostatting dynamics (which was tuned to the fast dynamics) to properly resonate with the slow system, and the result is poor ergodicity. This problem can either be viewed as an intrinsic aspect of the model, or a defect that should be rectified by the addition of more degrees of freedom in the slow dynamics (or an additional slow thermostatting bath).

Note that in more complicated applications arising in molecular simulation (e.g. [26]), sufficient ergodicity in the slow variables can typically be anticipated.

4.3. Benettin's diatomic Model. In this section, we will study a simplified diatomic model proposed by Benettin etc. in [4], which is subject to the following

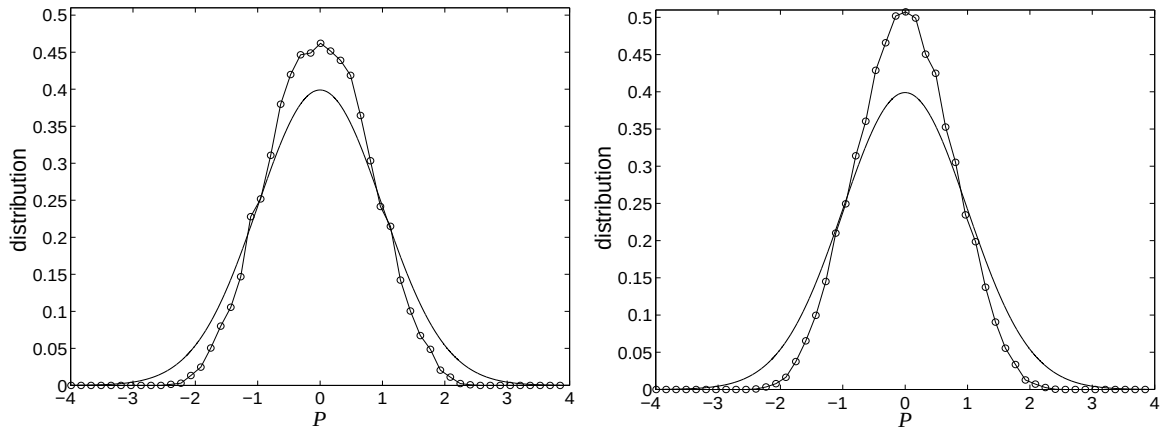

FIG. 4.5. *The distribution of the slow momentum P for* ***GRA*** *method in the weak coupling case, 2M (left) and 5M (right) time steps with $\delta t = 0.03$.*

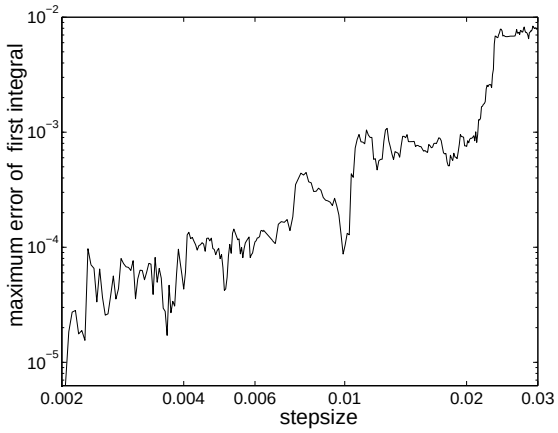

FIG. 4.6. *A log-log diagram of the maximum error of first integral $s\triangle\mathcal{H}$ versus stepsizes, for stepsizes 0.002—0.03 and time interval* $[0, 200]$.

Hamiltonian:

$$H = \sum_{i=1}^{N} \frac{1}{2}(p_i^2/m + \pi_i^2/m + m\omega^2\xi_i^2) + \sum_{i=1}^{N+1} V(x_i + \xi_i - x_{i-1} - \xi_{i-1}), \tag{4.2}$$

where V is the interaction potential energy, chosen as

$$V(r) = V_0 \frac{\exp(-(r/\sigma)^2)}{r/\sigma}. \tag{4.3}$$

In this paper, we chose $\omega = 10, V_0 = 1, \sigma = 1$ and use the dimensionless unit for time t. We define the vibrational energy as

$$\mathcal{E} = \frac{1}{2}\sum_{i=1}^{N}(\pi_i^2/m + m\omega^2\xi_i^2). \tag{4.4}$$

We outline three cases to test thermostatting issues related to Benettin's model.

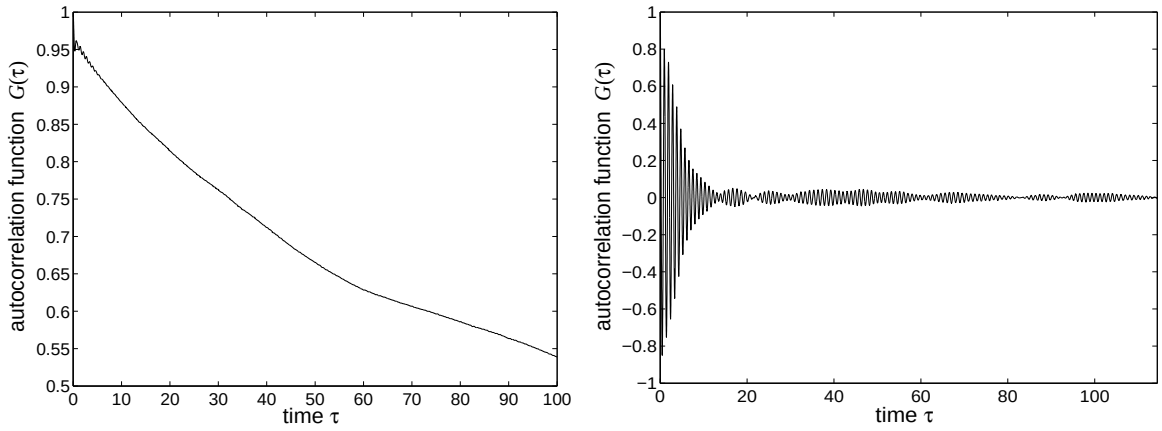

FIG. 4.7. *Fluctuation of vibrational energy for Benettin's model without thermostatting* **(a)** *and with thermostatting* **(b)**.

4.3.1. Mixing. We set up the initial data according to equipartition and considered the evolution of the system in the absence of any thermostatting device. The reversible averaging numerical method [24] has been used. In Figure 4.7 **(a)**, we see that the correlation funtion of fluctuation of the vibrational energy, as measured by the quantity

$$G(\tau) = \frac{\overline{\mathcal{E}(t)\mathcal{E}(t+\tau)} - \overline{\mathcal{E}(t)}^2}{\overline{\mathcal{E}(t)^2} - \overline{\mathcal{E}(t)}^2}, \tag{4.5}$$

where $\overline{x(t)}$ represents the temporal average of a function $x(t)$, decreases very slowly, coinciding precisely with the observations of [4].

Next, we applied partial thermostatting only to the vibrational variables by use of a Nosé-Poincaré chain. The resulting rapid mixing is illustrated in Figure 4.7 **(b)**, where the initial oscillation of correlation function implicates the frequent appreciable change of vibrational energy within a short time interval, and later long-time small fluctuation of correlation function can be explained by the weak effect from the translational degrees of freedom.

4.3.2. Thermal equilibration of vibrational degrees of freedom. From the above discussion, in Benettin's model, the fluctuation of vibrational energy is slow, so that we would expect the thermal equilibration of the vibrational components can't be attained even after a long time simulation if the initial data are not equilibrated at the proper temperature. To test this, we set up the initial vibrational energy corresponding to temperature $k_BT = 0.2$, while setting the initial translational kinetic energy to $k_BT = 0.1$. The translational and vibrational variables themselves relax to the equilibrium with different temperatures, respectively, in a long time interval simulation, as shown in Figure 4.8.

When the partial thermostatting (**PTD-III**, desired temperature $k_BT = 0.1$), is applied to the vibrational degrees of freedom, the results are shown in Figure 4.9. We observe that the vibrational variables tend to equilibrate at the target temperature.

4.3.3. The thermal equilibration of the whole system. From Figure 4.8 **(a)**, we notice that the translational degrees of freedom go into thermal equilibrium

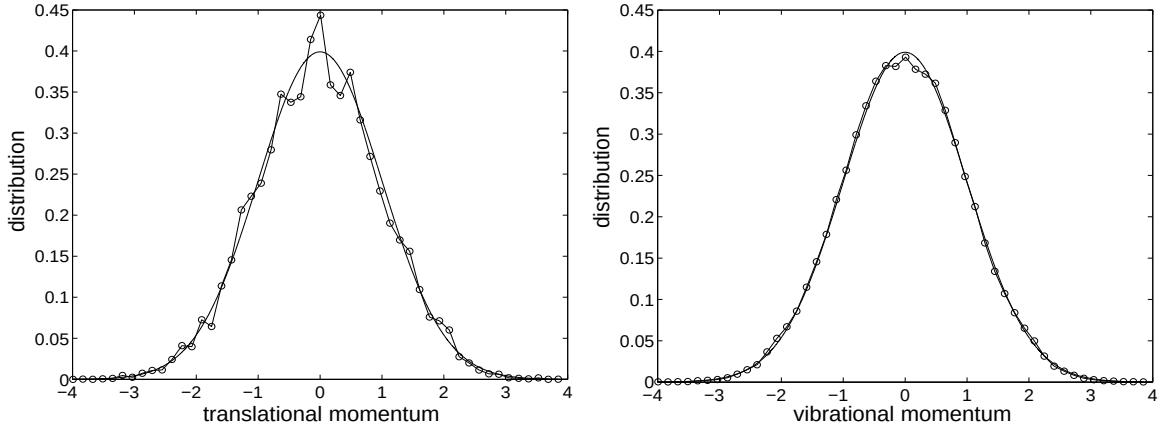

FIG. 4.8. *The distribution function of first translational* **(a)** *and vibrational* **(b)** *momentum for Benettin's model, with approximate equilibrated temperature* $k_BT = 0.0854$ *and* $k_BT = 0.1802$ *respectively, 4M time steps,* $\delta t = 0.05$.

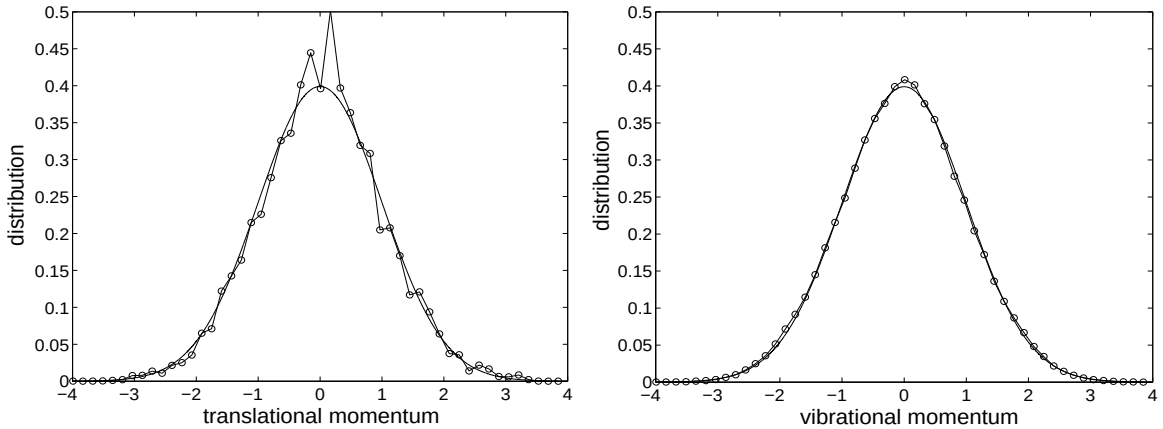

FIG. 4.9. *The distribution function of first translational* **(a)** *and vibrational* **(b)** *momentum with partial thermostatting of vibrational DOF,* $k_BT = 0.1$*, 4M time steps,* $\delta t = 0.05$.

slowly due to the lack of resonance between them. We therefore thermostat the translational variables only, and set up the initial data according to equipartition for all variables. Here we have employed the reversible averaging method in [24] for the system **PTD-I**. The final results for distribution functions are shown in Figure 4.10, which demonstrate that the whole system has been well equilibrated at temperature $k_BT = 0.1$.

5. Conclusion. In this paper, we have proposed a general framework of projective thermostatting dynamics for multiscale problems. Using these ideas, we are able to flexibly introduce canonical sampling over particular components while preserving physically relevant multiscale structural characteristics of the application and maintain these characteristics in the design of efficient numerical algorithms. Certain classes of problems with fast and slow variable separation were examined in detail. Moreover, a method has been proposed for following the slow evolution in a nonequi-

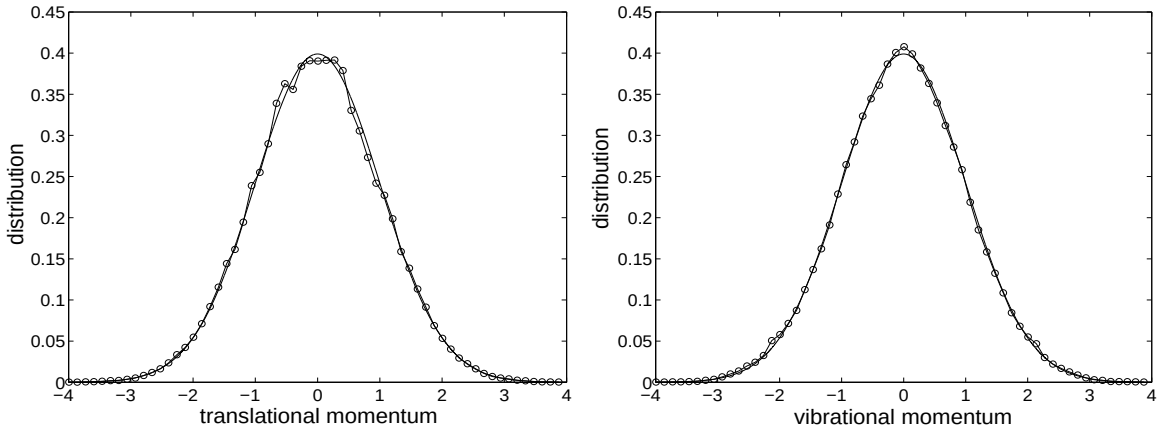

FIG. 4.10. *The distribution function of first translational* **(a)** *and vibrational* **(b)** *momentum with partial thermostatting of translational DOF,* $k_BT = 0.1$*, 6M time steps,* $\delta t = 0.05$*.*

librium setting, where only the fast degrees of freedom are assumed to be in equilibrium. The sampling properties of these new formulations were tested in numerical experiments using an enhanced "reversible averaging" scheme and a Nosé-Poincaré chain. Construction of a projective Nosé-Hoover dynamics with properties such as Galilean invariance and time-symmetry has also been described, although not yet tested in numerical experiments. We expect that the modeling and numerical computing techniques described in this paper may be of use in a variety of applications, such as models for material with defects where the physical domain is divided into a detailed atomistic model and a coarse-grained part, and for biomolecules with stiff potential terms to study nonequilibrium processes and the flow of energy or thermalization effects among different degrees of freedom. Stochastic modeling, e.g., Langevin or dissipative particle dynamics (**DPD**), may also be combined with the projection technique in order to introduce the thermal fluctuation and dissipation as needed. We will continue to explore these issues in forthcoming papers.

Appendix A. Canonical Phase Transformation with Nosé-Hoover Thermostatting. As used in [30], we define a symplectic[2] phase transformation as follows

$$\bar{q}_1 = \mathcal{U}(q), \tag{A.1}$$

$$\bar{q}_2 = b(q), \tag{A.2}$$

$$G^T\bar{p}_1 + B^T\bar{p}_2 = p, \tag{A.3}$$

where

$$B = b'(q). \tag{A.4}$$

In this way, we can obtain the transformed Hamiltonian function as

$$H_{trans} = \frac{\bar{p}_1^T G G^T \bar{p}_1}{2} + \frac{\bar{p}_2^T B B^T \bar{p}_2}{2} + V(\bar{q}_1, \bar{q}_2) + \sigma q_1^T e, \tag{A.5}$$

[2]The symplecticness of the specified transformation can be easily verified by checking $dq \wedge dp = d\bar{q} \wedge d\bar{p}$

and

$$e = (1, 1, \cdots, 1)^T, \bar{p} = (\bar{p}_1^T, \bar{p}_2^T)^T, \bar{q} = (\bar{q}_1^T, \bar{q}_2^T)^T. \tag{A.6}$$

We can apply Nosé dynamics to this transformed system, which is subject to the Hamiltonian

$$\mathcal{H}_{TN} = \frac{\tilde{p}_1^T G G^T \tilde{p}_1}{2s^2} + \frac{\bar{p}_2^T B B^T \bar{p}_2}{2} + V(\bar{q}_1, \bar{q}_2) + \sigma q_1^T e + \frac{\pi^2}{2\mu} + g_f k_B T \ln s. \tag{A.7}$$

It is very easy to prove that the dynamics recover the canonical ensemble distribution. Obviously, in this dynamics, the subsystem $(\bar{q}_1, \tilde{p}_1)$ has a virtual time scale and can be transformed to the real time scale by a time transformation applied to the subsystem $(\bar{q}_1, \tilde{p}_1)$ only. Combined with a coordinate transformation $\bar{p}_1 = \tilde{p}_1/s$, a variant of Nosé-Hoover dynamics is then obtained:

$$\dot{\bar{q}}_1 = G G^T \bar{p}_1, \tag{A.8}$$

$$\dot{\bar{q}}_2 = B B^T \bar{p}_2, \tag{A.9}$$

$$\dot{\bar{p}}_1 = -\nabla_{\bar{q}_1}(V + \sigma q_1^T e + K) - \frac{\xi}{\mu}\bar{p}_1, \tag{A.10}$$

$$\dot{\bar{p}}_2 = -\nabla_{\bar{q}_2}(V + K), \tag{A.11}$$

$$\dot{\xi} = \bar{p}_1^T G G^T \bar{p}_1 - g_f k_B T, \tag{A.12}$$

which can be rewritten in a compact form

$$\dot{\bar{Y}} = J \nabla_{\bar{Y}} \mathcal{H}_{trans} - \frac{\xi}{\mu} \begin{pmatrix} 0 \\ 0 \\ \bar{p}_1 \\ 0 \end{pmatrix}, \tag{A.13}$$

$$\dot{\xi} = \bar{p}_1^T G G^T \bar{p}_1 - g_f k_B T, \tag{A.14}$$

Where

$$K = \frac{\bar{p}_1^T G G^T \bar{p}_1}{2} + \frac{\bar{p}_2^T B B^T \bar{p}_2}{2}, \tag{A.15}$$

$$\bar{Y} = (\bar{q}^T, \bar{p}^T)^T. \tag{A.16}$$

The coordinates $(\bar{q}, \bar{p})$ are only used for theoretical purposes. To reformulate the above dynamics in terms of the original coordinate (p, q), we should re-apply the symplectic transformation defined by (A.1)-(A.3). Suppose

$$\phi = \frac{\partial(q,p)}{\partial(\bar{q},\bar{p})} \triangleq \frac{\partial Y}{\partial \bar{Y}} = \begin{pmatrix} \frac{\partial q}{\partial \bar{q}} & \frac{\partial q}{\partial \bar{p}} \\ \frac{\partial p}{\partial \bar{q}} & \frac{\partial p}{\partial \bar{p}} \end{pmatrix}, \tag{A.17}$$

then we get

$$\begin{aligned}\frac{dY}{dt} &= \left(\frac{\partial Y}{\partial \bar{Y}}\right)^T \frac{d\bar{Y}}{dt} \\ &= \phi^T \left(J\nabla_{\bar{Y}} \mathcal{H}_{trans} - \frac{\xi}{\mu} \begin{pmatrix} 0 \\ 0 \\ \bar{p}_1 \\ 0 \end{pmatrix} \right) \\ &= J\nabla_Y \mathcal{H}_{trans} - \frac{\xi}{\mu} \phi^T \begin{pmatrix} 0 \\ 0 \\ \bar{p}_1 \\ 0 \end{pmatrix}.\end{aligned}$$

Since

$$\frac{\partial p}{\partial \bar{q}} = 0, \frac{\partial p}{\partial \bar{p}} = \begin{pmatrix} G \\ B \end{pmatrix}, \tag{A.18}$$

we obtain dynamics in terms of (q, p)

$$\dot{q} = p, \tag{A.19}$$

$$\dot{p} = -\nabla_q (V + \sigma U) - \frac{\xi}{\mu} \mathcal{A} p, \tag{A.20}$$

$$\dot{\xi} = p^T \mathcal{A} p - g_f k_B T. \tag{A.21}$$

Subsequently, applying the symplectic transformation $p \to M^{1/2} p, q \to M^{-1/2} q$, the projection operator can be rewritten as

$$\mathcal{A} = M^{-1/2} G^T (G M^{-1} G^T)^{-1} G M^{-1/2}, \tag{A.22}$$

and the dynamics become the type of **PTD-II**:

$$\dot{q} = M^{-1} p, \tag{A.23}$$

$$\dot{p} = -\nabla_q (V + \sigma U) - \frac{\xi}{\mu} M^{1/2} \mathcal{A} M^{-1/2} p, \tag{A.24}$$

$$\dot{\xi} = p^T M^{-1/2} \mathcal{A} M^{-1/2} p - g_f k_B T. \tag{A.25}$$

Define

$$\mathcal{P} = M^{1/2} \mathcal{A} M^{-1/2} = G^T (G M^{-1} G^T)^{-1} G M^{-1}, \tag{A.26}$$

which is still a projection operator but not orthogonal since the rescaling by mass matrix breaks the symmetry of the projection matrix.

Note that once we have established the suitable form of the coupling term $\frac{\xi}{\mu} \mathcal{A}(q) p$, as clarified here, the dynamics could be derived from the formulation of Bulgac and Kusnezov [8].

Appendix B. A Generalized Reversible Averaging Method for PTD-III. Our method is designed to retain two properties of the dynamics in the numerical method: time reversibility and volume preservation. In order to get time reversibility, we employ a symmetric composition of the vector field splitting as well as a symmetric

averaging procedure, as elaborated in [19]. For example, a vector field splitting can be defined by:

$$VF1: \qquad \dot{P} = -\nabla_Q V(q,Q)$$

$$VF2: \qquad \dot{Q} = M^{-1}P$$
$$\dot{y}_f = g(y_f, Q, P),$$

where y_f represents the vector of dynamical variables in the fast subdynamics. The symmetric averaging idea is that we can compute the fast subdynamics forward and backward in time with slow variables fixed at the symmetric time points, and then a modified vector field of the slow subdynamics, taken as the time average along the evolution of the fast subdynamics, can be used to propagate the slow subdynamics. Thus, we replace subsystem $VF1$ by

$$AVF1: \qquad \dot{P} = \langle -\nabla_Q V(q(t), Q)\rangle, \tag{B.1}$$

which is exactly the form of averaging dynamics known in astrophysics [1]. An on-the-fly time average during the numerical integration is employed in place of the global time average used in theory, and mimics that averaging principle locally. We suppose that the symmetric (forward and backward) averaging idea will result in two symmetric subsystems $AVF1^+$ and $AVF1^-$ respectively. Thus, we can formulate our numerical integrator as

$$\phi^{\delta t} = \phi^{\delta t/2}_{AVF1^-} \circ \phi^{\delta t}_{VF2} \circ \phi^{\delta t/2}_{AVF1^+}. \tag{B.2}$$

If there is a strong coupling between the fast subdynamics and slow momenta P, as we expect in **PTD**, the averaging procedure can't be used before we solve the subsystem $AVF1^-$ because the slow momenta P^1 is not available. We have considered several possible ways of resolving this difficulty.

One method is to define P^1 implicitly by

$$P^1 = P^{1/2} - \delta t/2\langle -\nabla_Q V(q(t), Q^1), \rangle$$

where $q(t)$ is now obtained by solving backwards in time from q^1, p^1, with $Q = Q^1$ and $P = P^1$. Unfortunately, this method leads to an expensive iteration (with multiple fast solves) to determine P^1.

The P-dependence in the fast dynamics is a consequence of using a Nosé-Poincaré approach within **PTD**, which is likely to improve stability. However, nothing prevents the use of a combination method whereby Nosé-Hoover dynamics is employed to compute fast dynamics during the averaging stage, whereas Nosé-Poincaré is still the basis for fast propagation. This scheme, while introducing additional complexity, has many potential advantages. In particular it can be shown to be not only time-reversible but also volume preserving.

For simplicity, we have implemented third alternative scheme based on a system of *dual slow variables*. An independent procedure can be employed to compute a dual variable $\bar{P}$, distinguished from the propagation solution P. The simplest technique is to use an algebraic relation such as

$$G(\bar{P}^{n+1}, \bar{P}^n, P^{n+1/2}) = 0, \tag{B.3}$$

where G is symmetric with respect to the exchange of $\bar{P}^{n+1}$ and $\bar{P}^n$. Given $\bar{P}^0$, $\bar{P}^n$ can be obtained by solving (B.3). We implemented this scheme, but as it behaved poorly. An improved approach was based on updating $\bar{P}$ from an alternative solution of its governing differential equation, i.e. by a separate symmetric numerical solution of

$$\dot{P} = -\nabla V(q(t), Q^{n+1/2}), \tag{B.4}$$

which actually uses the available fast propagation. This method performed well and was used in our experiments.

Appendix C. A Nosé-Poincaré Chain within PTD-III. To generate ergodic sampling, we used the following Nosé-Poincaré chain [33, 25] for the fast subdynamics while considering the slow variables as resolved time-dependent quantities,

$$\mathcal{H}^{NP-chain} = s(\frac{P^T P}{2M} + \mathcal{H}^{Nosé-chain} - \mathcal{H}_0), \tag{C.1}$$

where

$$\begin{aligned}\mathcal{H}^{Nosé-chain} = &\frac{p^2}{2ms_1^2} + g_f K_B T \ln(s_1) + \sum_{j=1}^{L-1} \frac{\pi_j^2}{2Tm_j s_{j+1}^2} \\ &+\frac{\pi_L^2}{2Tm_L} + \sum_{j=2}^{L}(K_B T \ln(s_j) + \frac{(1-s_j)^2}{Rm_j}) + V(q,Q).\end{aligned} \tag{C.2}$$

The various coefficients Rm_i, Tm_i can be chosen as suggested in [33].

We construct a "new" Hamiltonian splitting as follows:

$$\mathcal{H}^{NP-chain} = \sum_{j=0}^{L+1} \mathcal{H}_j, \tag{C.3}$$

$$\mathcal{H}_0 = s_1(\frac{p^2}{2ms_1^2} + g_f K_B T \ln(s_1)), \tag{C.4}$$

$$\mathcal{H}_1 = s_1(\frac{\pi_1^2}{2Tm_1 s_2^2} + K_B T \ln(s_2) + \frac{(1-s_2)^2}{Rm_2}), \tag{C.5}$$

$$\mathcal{H}_i = s_1(\frac{\pi_i^2}{2Tm_i s_{i+1}^2} + K_B T \ln(s_{i+1}) + \frac{(1-s_{i+1})^2}{Rm_{i+1}}), 2 \leqq i \leqq L-1, \tag{C.6}$$

$$\mathcal{H}_L = s_1 \frac{\pi_L^2}{2Tm_L}, \tag{C.7}$$

$$\mathcal{H}_{L+1} = s_1(\frac{P^2}{2M} + V(q,Q) - \mathcal{H}_0). \tag{C.8}$$

The Hamiltonian $\mathcal{H}_1$ can be integrated by use of a generalized leap-frog method [6], and the other Hamiltonians can be solved analytically. A numerical integrator can be constructed as

$$\phi^{\delta t} = \phi_{\mathcal{H}_0}^{\delta t/2} \circ \cdots \circ \phi_{\mathcal{H}_L}^{\delta t/2} \circ \phi_{\mathcal{H}_{L+1}}^{\delta t} \circ \phi_{\mathcal{H}_L}^{\delta t/2} \circ \cdots \circ \phi_{\mathcal{H}_0}^{\delta t/2}. \tag{C.9}$$

Acknowledgments The authors were supported by The UK Engineering and Physical Sciences Research Council under Grant No. EPSRC GR/R03259. We thank

Chris Sweet (University of Leicester) for helping to explain the use of the Nosé-Poincaré chain, Simone Melchionna (INFN-Rome) for reading and commenting on a draft of the article. We are also grateful for the valuable discussions with Brian Laird (University of Kansas) and Qun Ma (New Jersey Institute of Technology). A preliminary version of this paper was presented at the Workshop "Invariance and Model Reduction for Multiscale Phenomena", **ETH**, Zurich, August 26 - August 29, 2003.

REFERENCES

[1] V. I. Arnold, V. V. Kozlov, and A. I. Neishtadt, *Mathematical Aspects of Classical and Celestial Mechanics*, Springer-Verlag, 1997.
[2] E. J. Barth, B. B. Laird, and B. J. Leimkuhler, *Generating Generalized Distributions from Dynamical Simulation*, J. Chem. Phys., 118 (2003), pp. 5759–5768.
[3] P. F. Batcho and T. Schlick, *Special Stability Advantages of Position-Verlet over Velocity-Verlet in Multiple Time Step Integration*, J. Chem. Phys., 115 (2001), pp. 4019–4029.
[4] G. Benettin, L. Galgani, and A. Giorgilli, *Exponential Law for The Equilibration Times among Translational and Vibrational Degrees of Freedom*, Phys. Lett. A, 120 (1987), pp. 23–27.
[5] L. Boltzmann, *On Certain Questions of the Theory of Gases*, Nature, 51 (1895), pp. 413–415.
[6] S. D. Bond, B. J. Leimkuhler, and B. B. Laird, *The Nosé-Poincaré Method for Constant Temperature Molecular Dynamics*, J. Comp. Phys., 151 (1999), pp. 114–134.
[7] F. A. Bornemann, *Homogenization in Time of Singularly Perturbed Conservative Mechanical Systems*, Lecture Notes in Mathematics Vol. 1687, Springer-Verlag, 1998.
[8] A. Bulgac and D. Kusnezov, *Canonical Ensemble Averages from Pseudomicrocanonical Dynamics*, Phys. Rev. A, 42 (1990), pp. 5045–5048.
[9] K. Cho and J. D. Joannopoulos, *Constant Temperature Molecular Dynamics with Momentum Conservation*, Phys. Rev. E, 47 (1993), pp. 3145–3151.
[10] S. Cirilli, E. Hairer, and B. J. Leimkuhler, *Asymptotic Error Analysis of the Adaptive Verlet Method*, BIT, 39 (1999), pp. 25–33.
[11] D. J. Evans and G. P. Morris, *Statistical Mechanics of Nonequilibrium Liquids, Academic Press*, London, 1990.
[12] D. Givon, R. Kupferman, and A. M. Stuart, *Extracting macroscopic dynamics: model problems and algorithms*, Nonlinearity, 17 (2004), pp. R55–127.
[13] E. Hairer and Ch. Lubich, *Long-time Energy Conservation of Numerical Methods for Oscillatory Differential Equations*, SIAM J. Numer. Anal., 38 (2000), pp. 414–441.
[14] W. G. Hoover, *Canonical Dynamics: Equilibrium Phase-space Distributions*, Phys. Rev. A, 31 (1985), pp. 1695–1697.
[15] J. A. Izaguirre, S. Reich, and R. D. Skeel, *Longer Time Steps for Molecular Dynamics*, J. Chem. Phys., 110 (1999), pp. 9853–9864.
[16] J. H. Jeans, *On the Vibrations set up in Molecules by Collisions*, The London, Edinburgh, and Dublin Philosophical Magazine and Journal of Science, 6th Series, August 1903, pp. 279–286.
[17] J. H. Jeans, *On the Partition of Energy between Matter and Ether*, The London, Edinburgh, and Dublin Philosophical Magazine and Journal of Science, 10th Series, July 1905, pp. 91–97.
[18] J. Jellinek and R. S. Berry, *Generalization of Nosé Isothermal Molecular Dynamics*, Phys. Rev. A, 38 (1988), pp. 3069–3072.
[19] Z. Jia and B. J. Leimkuhler, *A Parallel Multiple Time-scale Reversible Integrator for Dynamics Simulation*, J. Fut. Gen. Comp. Sys., 19 (2003), pp. 415–424.
[20] W. Just, K. Gelfert, N. Baba, A. Riegert, and H. Kantz, *Elimination of Fast Chaotic Degrees of Freedom: On the Accuracy of the Born Approximation*, J. Statist. Phys., 112 (2001), pp. 277–292.
[21] W. Just, H. Kantz, C. Renbeck, and M. Helm, *Stochastic Modeling: Replacing Fast Degrees of Freedom by Noise*, J. Phys. A, 34 (2001), pp. 3199–3213.
[22] D. Kusnezov, *Diffusive Aspects of Global Demons*, Phys. Lett. A, 166 (1992), pp. 315–320.
[23] B. J. Leimkuhler, S. Reich and R. D. Skeel, *Integration Methods for Molecular Dynamics*, in Jill P. Mesirov, Klaus Schulten, De Witt Sumners, editors, Mathematical Approaches to Biomolecular Structure and Dynamics, Vol. 82 of IMA Volumes in Mathematics and its Applications, 161–185, Springer-Verlag, 1996.

[24] B. J. Leimkuhler and S. Reich, *A Reversible Averaging Integrator for Multiple Time-scale Dynamics*, J. Comput. Phys., 171 (2001), pp. 95–114.
[25] B. J. Leimkuhler and C. R. Sweet, *A Hamiltonian Formulation for Recursive Multiple Thermostats in a Common Timescale*, SIAM J. of Applied Dynamical Systems, to appear.
[26] Q. Ma and J. A. Izaguirre, *Targeted Mollified Impulse: A Multiscale Stochastic Integrator for Long Molecular Dynamics Simulations*, MMS, 2 (2003), pp. 1–21.
[27] G. J. Martyna, M. E. Tuckerman and M. L. Klein, *Nose-Hoover Chains: The Canonical Ensemble via Continuous Dynamics*, J. Chem. Phys., 97 (1992), pp. 2635–2643.
[28] P. Mazur and I. Oppenheim, *Molecular Theory of Brownian Motion*, Physica, 50 (1970), pp. 241–258.
[29] S. Nosé, *Constant Temperature Molecular Dynamics Methods*, Progr. Theoret. Phys. Suppl., 103 (1991), pp. 1–46.
[30] S. Reich, *Smoothed Dynamics of Highly Oscillatory Hamiltonian Systems*, Physica D, 89 (1995), pp. 28–42.
[31] Ch. Schütte and F. A. Bornemann, *Homogenization Approach to Smoothed Molecular Dynamics*, Nonlinear Analysis, Theory, Methods and Applications, 30 (1997), pp. 1805–1814.
[32] J. B. Sturgeon and B. B. Laird, *Symplectic Algorithm for Constant-pressure Molecular-dynamics using A Nose-Poincare Thermostat*, J. Chem. Phys., 112 (2000), pp. 3474–3482.
[33] C. R. Sweet and B. J. Leimkuhler, *The Canonical Ensemble via Symplectic Integrators using Nosé and Nosé-Poincaré Chains*, J. Chem. Phys., 121 (2004), pp. 108–116.
[34] E. B. Tadmor, M. Ortiz and R. Phillips, *Quasicontinuum Analysis of Defects in Solids*, Philos. Mag. A, 73 (1996), pp. 1529–1563.
[35] M. Tuckerman, B. J. Berne and A. Rossi, *Molecular Dynamics for Multiple Time Scales: Systems with Disparate Masses*, J. Chem. Phys., 94 (1991), pp. 1465–1469.
[36] N. G. Van Kampen and I. Oppenheim, *Brownian Motion as A Problem of Eliminating Fast Variables*, Phys. A, 38 (1986), pp. 231–248.
[37] R. Zwanzig, *Ensemble Method in the Theory of Irreversibility*, J. Chem. Phys., 33 (1960), pp. 1338–1341.